

ARMY RESEARCH LABORATORY



Low-Cost Production of Photonic Bandgap Materials Through Bubbling

by Daniel J. O'Brien and Eric D. Wetzel

ARL-TR-4277

September 2007

NOTICES

Disclaimers

The findings in this report are not to be construed as an official Department of the Army position unless so designated by other authorized documents.

Citation of manufacturer's or trade names does not constitute an official endorsement or approval of the use thereof.

Destroy this report when it is no longer needed. Do not return it to the originator.

Army Research Laboratory

Aberdeen Proving Ground, MD 21005-5069

ARL-TR-4277

September 2007

Low-Cost Production of Photonic Bandgap Materials Through Bubbling

**Daniel J. O'Brien and Eric D. Wetzel
Weapons and Materials Research Directorate, ARL**

REPORT DOCUMENTATION PAGE			<i>Form Approved</i> OMB No. 0704-0188		
Public reporting burden for this collection of information is estimated to average 1 hour per response, including the time for reviewing instructions, searching existing data sources, gathering and maintaining the data needed, and completing and reviewing the collection information. Send comments regarding this burden estimate or any other aspect of this collection of information, including suggestions for reducing the burden, to Department of Defense, Washington Headquarters Services, Directorate for Information Operations and Reports (0704-0188), 1215 Jefferson Davis Highway, Suite 1204, Arlington, VA 22202-4302. Respondents should be aware that notwithstanding any other provision of law, no person shall be subject to any penalty for failing to comply with a collection of information if it does not display a currently valid OMB control number. PLEASE DO NOT RETURN YOUR FORM TO THE ABOVE ADDRESS.					
1. REPORT DATE (DD-MM-YYYY) September 2007		2. REPORT TYPE Final		3. DATES COVERED (From - To) January 2003–January 2005	
4. TITLE AND SUBTITLE Low-Cost Production of Photonic Bandgap Materials Through Bubbling			5a. CONTRACT NUMBER		
			5b. GRANT NUMBER		
			5c. PROGRAM ELEMENT NUMBER		
6. AUTHOR(S) Daniel J. O'Brien and Eric D. Wetzel			5d. PROJECT NUMBER 611102.AH42		
			5e. TASK NUMBER		
			5f. WORK UNIT NUMBER		
7. PERFORMING ORGANIZATION NAME(S) AND ADDRESS(ES) U.S. Army Research Laboratory ATTN: AMSRD-ARL-WM-MA Aberdeen Proving Ground, MD 21005-5069			8. PERFORMING ORGANIZATION REPORT NUMBER ARL-TR-4277		
9. SPONSORING/MONITORING AGENCY NAME(S) AND ADDRESS(ES)			10. SPONSOR/MONITOR'S ACRONYM(S)		
			11. SPONSOR/MONITOR'S REPORT NUMBER(S)		
12. DISTRIBUTION/AVAILABILITY STATEMENT Approved for public release; distribution is unlimited.					
13. SUPPLEMENTARY NOTES					
14. ABSTRACT Photonic bandgap materials (PBGs) prevent the propagation of electromagnetic waves across certain wavelengths—the so-called bandgap. This behavior is the result of periodic variations in the material's dielectric constant, with the location of the bandgap as a function of the spacing between dielectric features. PBGs show great promise in optoelectronics as waveguides and in sensors. Unfortunately, the large-scale production of PBGs is difficult. This report proposes a simple low-cost method for PBGM production. A device has been constructed that produces micrometer-sized, monodisperse bubbles that can be assembled into a crystal lattice by surface tension. The bubble crystals can be solidified and preserved using an aqueous acrylamide monomer solution as the medium for bubbling.					
15. SUBJECT TERMS photonic bandgap, bubble, foam, self-assembly, hydrogel					
16. SECURITY CLASSIFICATION OF:			17. LIMITATION OF ABSTRACT UL	18. NUMBER OF PAGES 38	19a. NAME OF RESPONSIBLE PERSON Daniel J. O'Brien
a. REPORT UNCLASSIFIED	b. ABSTRACT UNCLASSIFIED	c. THIS PAGE UNCLASSIFIED			19b. TELEPHONE NUMBER (Include area code) 410-306-0843

Contents

List of Figures	iv
1. Introduction	1
1.1 Photonic Bandgap Materials	1
1.2 Motivation	2
1.3 Background – Bubbling Techniques	3
1.4 Foam Background	3
2. Experimental	6
2.1 Bubbling Device.....	6
2.2 Materials and Procedure.....	9
2.2.1 Aqueous Foams	9
2.2.2 Solid Foams	9
2.2.3 Emulsions	11
3. Results and Discussion	11
3.1 Aqueous Foams	11
3.2 Solid Foam	16
3.2.1 Polymer	16
3.2.2 Ceramic	19
3.3 Emulsions	20
4. Summary and Conclusions	20
5. References	23
Appendix. Additional Images	27
Distribution List	31

List of Figures

Figure 1. Schematic of photonic bandgap effect. All wavelengths of a broadband light beam are transmitted through the structure except for a narrow band near the lattice parameter of the PBGM.	1
Figure 2. Schematic of bubbling device.	6
Figure 3. Liquid flow rate as a function of orifice diameter at limiting Weber numbers for stable bubbling.	7
Figure 4. Bubbler with connected tubing and fittings.	8
Figure 5. Schematic of technique for producing solid acrylamide foams.	10
Figure 6. View of bubble fountain from above (75- μm orifice).	12
Figure 7. Bubbles produced with 50- μm orifice ($Q_l = Q_g = 250 \mu\text{L}/\text{min}$).	13
Figure 8. Bubbles produced with 35- μm orifice ($Q_l = 64 \mu\text{L}/\text{min}$, $Q_g = 32 \mu\text{L}/\text{min}$).	13
Figure 9. Bubbles produced with 35- μm orifice ($Q_l = Q_g = 64 \mu\text{L}/\text{min}$).	14
Figure 10. Bubbles produced with 35- μm orifice ($Q_l = 64 \mu\text{L}/\text{min}$, $Q_g = 8 \mu\text{L}/\text{min}$).	14
Figure 11. Evidence of ordering through three bubble layers. Scale unknown.	15
Figure 12. Bubble size control through relative flow rate.	15
Figure 13. Acrylamide monodisperse polymeric foam after processing with technique no. 1. ...	17
Figure 14. Acrylamide monodisperse polymeric foam after processing with technique no. 2 (lower magnification).	17
Figure 15. Acrylamide monodisperse polymeric foam after processing with technique no. 2 (higher magnification).	18
Figure 16. Acrylamide foam. Micrograph taken with microscope focused on the first layer of bubbles, nearest the camera.	18
Figure 17. Acrylamide foam. Micrograph taken with microscope focused on the second layer of bubbles.	19
Figure 18. Silica gel produced from acrylamide template (sample 1).	19
Figure 19. Silica gel produced from acrylamide template (sample 2).	20
Figure 20. Ordering of monodisperse water-octane emulsion stabilized with SDS.	21
Figure A-1. Aqueous bubbles produced with 50- μm orifice ($Q_l = Q_g = 250 \mu\text{L}/\text{min}$). Fountain is shown at bottom-right of frame.	28
Figure A-2. Aqueous bubbles produced with 50- μm orifice ($Q_l = 250 \mu\text{L}/\text{min}$, $Q_g = 16 \mu\text{L}/\text{min}$).	28
Figure A-3. Acrylamide monodisperse polymeric foam.	29
Figure A-4. Acrylamide monodisperse polymeric foam (high magnification).	29
Figure A-5. Acrylamide monodisperse polymeric foam. Image shows preservation of cubic structure in first layer.	30

1. Introduction

1.1 Photonic Bandgap Materials

Materials with spatial variation in dielectric properties have unusual optical properties when the period of variation is close to the wavelength of light. Along the axis of periodicity, the variation can give rise to a “stop band”—a portion of the electromagnetic spectrum that is forbidden from propagation through the medium. If the material is in the form of a stack (a one-dimensional variation in dielectric properties), it prevents propagation of certain frequencies through the thickness. On the other hand, a material with three-dimensional (3-D) periodicity can have a complete photonic band gap, preventing propagation of certain frequencies in all directions (figure 1). Such materials are called photonic bandgap materials (PBGMs) (1). This unique optical property holds prospects for many exciting applications, including the development of computers that process photons instead of electrons, which allows for computation at speeds thousands of times faster than is possible with current technology (2). These optical computers will likely include waveguides, light-emitting diodes, and transistors based on PBGMs. In sensor applications, a PBGM constructed out of a material that swells or shrinks in response to an environmental change results in a detectable shift in the bandgap. Additionally, PBGMs have also been used to tailor the optical and thermal (3) properties of surfaces (4).

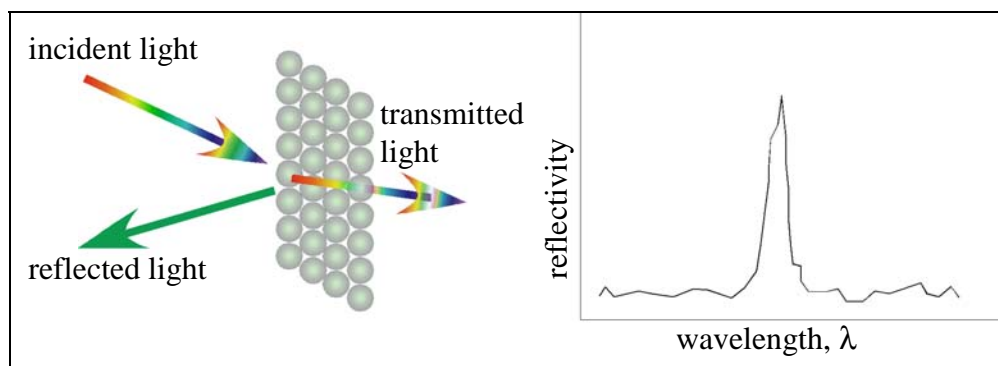


Figure 1. Schematic of photonic bandgap effect. All wavelengths of a broadband light beam are transmitted through the structure except for a narrow band near the lattice parameter of the PBGM.

The most efficient PBGMs—those that prevent propagation of the greatest proportion of incident energy over the widest bandgap—are composed of materials with a high index contrast. That is, the high and low index phases have significantly different indices of refraction. Also, the most efficient two-dimensional and 3-D structures require that the walls of the periodic structure are composed of the high index material. These requirements have led researchers to investigate techniques that produce so-called inverse opals—periodically arranged voids of air in a high index matrix.

Natural opals—crystals of submicrometer silica spheres—are formed under very special conditions over millions of years. In recent years, researchers have developed much faster techniques for producing 3-D structures for PBGMs. These methods include lithography, emulsion templating, holography, spin annealing, melt compression, and controlled drying.

Schroden et al. (4) produced opals through centrifugation of nanometer-sized, monodisperse polymethylmethacrylate spheres. The opals were then converted to inverse opals through infiltration of a sol gel precursor, followed by removal of the polymer spheres upon heating. Xu et al. (5) used a similar, spin annealing technique and larger spheres for infrared applications. Gates et al. (6) used a sedimentation technique that assembles monodisperse particles inside a special cell with sonication under flowing solvent. Srinivasarao et al. (7) formed 3-D hexagonal holes in a polymer film using the condensation of water droplets onto the surface of a volatile solvent/polymer solution. Evaporation of solvent and water resulted in a regular array of holes. Sharp et al. (8) used four interfering laser beams to expose a polymer photoresist film with a 3-D periodic pattern. Kondo et al. (9) also used an interference technique. Fink et al. (10) determined that block copolymers could be self-assembled into 3-D periodic arrays with photonic properties. Instead of using solid spheres as templates, Imhof and Pine (11) demonstrated the manufacture of photonic crystals using ordered monodisperse emulsions as templates. Ruhl et al. (12) synthesized monodisperse polystyrene-polymethylmethacrylate core-shell particles in a polyethylene acrylate matrix. The material was then manufactured into a thin film by compression—a high-shear process that resulted in ordering of the spheres.

1.2 Motivation

While many of these techniques are capable of producing high quality opals and inverse opals, they are generally not amenable to the production of large quantities of material. The lithographic techniques are too slow and require a significant capital investment. Techniques based on the sedimentation of monodisperse particles are also quite slow or require many steps. Furthermore, with emulsion polymerization (the technique used to produce the particles), it is difficult to manufacture monodisperse particles larger than $\sim 1.5 \mu\text{m}$ in diameter (13), which is too small to cover much of the infrared regime. PBGMs from monodisperse emulsions are simple to make once the emulsion is in hand. However, the monodisperse emulsions are generally made using a tedious fractionation process (14).

The goal of this work is to develop a technique that would overcome these deficiencies by using a scalable method with only a few steps to produce PBGMs from monodisperse bubbles in a curable fluid. Also, the technique should provide control of the bubble size over a wide range to enable precise manipulation of wavelengths from the visible through the far infrared. Furthermore, for a strong photonic bandgap effect, the final matrix material should have a high index of refraction.

The approach taken in producing PBGM structures through bubbling techniques can be divided into two major steps: monodisperse bubble production and foam crystal solidification. The remainder of this report discusses these aspects. First, several techniques for producing bubbles will be surveyed. One particularly promising technique used to produce aqueous foam crystals is discussed in greater detail. Then, methods for producing permanent solid foam crystals are discussed, and techniques for producing ordered polymer and ceramic foams are demonstrated. Finally, avenues for further study are discussed.

1.3 Background – Bubbling Techniques

There are several available techniques for mass-producing bubbles. As one example, a gas dissolved in a liquid at high pressure produces foam upon a sudden decrease in pressure. As another example, foaming agents produce bubbles through the decomposition (upon heating) of particles into carbon dioxide. As a third example, gas can be directly introduced into the liquid through an orifice, a technique called sparging.

Unfortunately, producing very small ($\sim 5\text{-}\mu\text{m}$) monodisperse bubbles with any of these techniques is difficult. The dissolved gas approach is not attractive—foams produced in this manner are generally polydisperse because bubbles that nucleate at different times have different sizes (15). Producing monodisperse foams from foaming agents requires a monodisperse foaming agent powder. Assuming that the volume of gas produced by the foaming agent is $200\times$ the size of the particle, monodisperse powders of less than $1\ \mu\text{m}$ would be needed to produce $5\text{-}\mu\text{m}$ bubbles. The sparging technique would require very small orifices, because the method produces bubbles that are always larger than the orifice itself (16).

Although it has not been demonstrated, it might be possible to produce monodisperse bubbles by modifying a vibrating orifice aerosol generator (VOAG) (17). A VOAG consists of a small orifice that is attached to a piezoceramic. The size of the monodisperse micrometer-sized droplets emerging from the orifice can be controlled by the frequency of vibration of the piezoceramics.

In this work, micrometer-sized monodisperse bubbles are produced using a method similar to sparging, except it involves the concentric flow of gas and liquid through a small orifice. In their peer-reviewed publication, Gañán-Calvo and Gordillo claim to have produced bubbles as small as $5\ \mu\text{m}$ (18) using the technique, and bubbles as small as $\sim 0.1\ \mu\text{m}$ have been claimed in the patent literature (19).

1.4 Foam Background

Once monodisperse bubbles have been produced and organized into a crystal lattice, the structure must be solidified and preserved without destroying the material's periodic structure. Unfortunately, liquid foams are inherently unstable, and their structure is constantly changing. Therefore, it is instructive to discuss three mechanisms by which foams evolve: drainage,

evaporation, and disproportionation. Foam drainage is the process of liquid at the top of the foam flowing toward the bottom. Newly formed foam, called a wet foam, is composed of spherical bubbles with films that have plenty of excess fluid. As the liquid drains, the bubbles become polyhedral in shape, and the foam is called a dry foam. When enough liquid drains from a film, it ruptures. Liquid can also be removed from the foam through evaporation, a source of further film-thinning and bubble-rupture. Disproportionation, driven by the pressure inside the bubbles, is the increase in the size of a bubble at the expense of an adjacent, smaller bubble. A force balance of internal pressure and surface tension on a bubble's film reveals that the pressure inside of a bubble must increase as radius decreases. This relationship drives the transport of gas from small bubbles to large bubbles.

Foams are not absolutely stable since their large surface area (compared to the unfoamed liquid) results in a large surface energy and a natural tendency of the system to decrease its energy through coarsening or film-rupture. However, simply minimizing the foam's surface energy by choosing a low surface tension liquid does not yield the most stable foams, since pure liquids do not foam. A bubble that rises to the surface of a pure liquid will quickly (in milliseconds) rupture because there is nothing to prevent its film from thinning and becoming unstable (20).

Foam films are usually stabilized by mixing a small amount of surfactant with the fluid. A surfactant (or surface-active agent) is a molecule with opposing hydrophilic and hydrophobic ends that, when in solution, preferably absorb at solvent-gas or solvent-oil interfaces and result in a decrease in surface tension (20). When a foam film is stretched, the local concentration of surfactant at the surface decreases, causing a local increase in the surface tension. This increase in local surface tension provides a restoring force to the film and inhibits further stretching. Also, surfactants can be used to create a charged double layer from the surfaces of adjacent bubbles. The electrostatic repulsion of two like-charged surfaces can prevent coalescence.

Polar liquids are often the best solvents for surfactants because they are compatible with the surfactant's hydrophilic end and tend to force the hydrophobic end to the interfaces (21). Therefore, water is often used as the solvent to produce stable foams.

In addition to using a surfactant, there are several steps that can be taken to increase the stability of foams. These include slowing down drainage, increasing film elasticity, decreasing gas transport across the bubbles' films, and increasing the thickness of the electrical double layer between the surfaces of a film (22). For example, additives that increase the bulk viscosity of the liquid will decrease the rate of drainage. Additives (such as some proteins) are surface-active and increase the surface viscosity of the film, inhibiting drainage (23). Similarly, methylcellulose ether is a surface-active agent that also provides bulk gelation at sufficient concentration in an aqueous solution. Since it is surface-active, it can gel the gas-liquid interface at very low concentration (0.01% by weight) (24). It has also been reported that monodisperse particles in the liquid can arrange themselves in the film and induce step-wise thinning of the film (25).

Additives with low vapor pressure can be used to inhibit evaporation of the liquid. Disproportionation can be overcome by producing bubbles with a gas that has a low solubility or a high diffusion constant with the liquid. Also, it has been demonstrated that disproportionation is slower in monodisperse foams (26).

The ultimate goal of this work is to produce periodic foams with the highest possible refractive index contrast. Since ceramic materials typically have the highest refractive indices, it is useful to explore pathways to the production of ceramic-ordered foams. In the remainder of the section, we will survey several techniques for ceramic foam production using the bubbler.

There are many techniques available for producing ceramic foams. Santos et al. (27) produced a zirconia foam from a sol gel solution of zirconyl chloride and sulfuric acid and a surfactant. Freon-11 was also mixed into the solution at high pressure, which produced a foam depressurization. Foams with spherical pores were produced with the surfactant Igepal-710. However, the viscosity of the sol that they used was quite high (~5000 cp). A special characteristic of the sol is that it produces a thermoreversible gel upon heating above ~27 °C. This might allow one to produce a foam at low temperature (where the sol has a low viscosity) and then heat it slightly to induce thermoreversible gelation, which would stabilize the foam until a permanent network is formed.

Wu et al. (28) also used direct foaming of a ceramic precursor, tetraethylorthosilicate (TEOS), to produce a foam. This precursor has a very low viscosity (~10 cp), which would make it amenable to foaming using the bubbler. However, an appropriate surfactant would be required to stabilize the ordered foam as the network develops. The process would likely be complicated by the evaporation of solvent, which could destroy bubbles.

Preceramic polymers are used to produce ceramic parts by heating the polymer to a temperature high enough to drive off the organics. The uncured polymers have fairly low viscosities (~80–150 cp) which might permit use in the bubbler. Foams of these materials have been produced by mixing them with a liquid blowing agent. Silicone surfactants are used for bubble stabilization.

Imhof and Pine (11) used a technique called emulsion templating to produce an ordered ceramic foam with potential applications as a PBGM. In this technique, a monodisperse oil-in-water emulsion is prepared and mixed with a water-soluble ceramic precursor. Centrifugation orders the emulsion. Then, a small amount of catalyst is added to promote gelation of the precursor around the oil droplets. A solvent is used to remove the oil droplets, and, finally, the part is fired to produce the ceramic foam. It is possible that this procedure could be scaled up. However, the production of the monodisperse emulsions is tedious.

2. Experimental

2.1 Bubbling Device

Figure 2 shows a schematic of the bubbler and the production of the monodisperse bubbles. The device consists of a capillary of flowing gas that is concentric with a tube of flowing liquid. The exit of the capillary is just upstream of a small orifice. As the gas exits the capillary, it is drawn into and forced through the orifice by the flowing liquid. The absolute instability of the ligament at the exit of the orifice is unaffected by external conditions, and it causes the ligament to break at an extremely regular frequency, which produces monodisperse bubbles (29). The absolute instability is a result of the Kelvin-Helmholtz instability, which causes regular vortices to develop because of shear between parallel flowing fluids. The vortices result in a thinning of the gas filament, which is eventually pinched off due to the capillary instability.

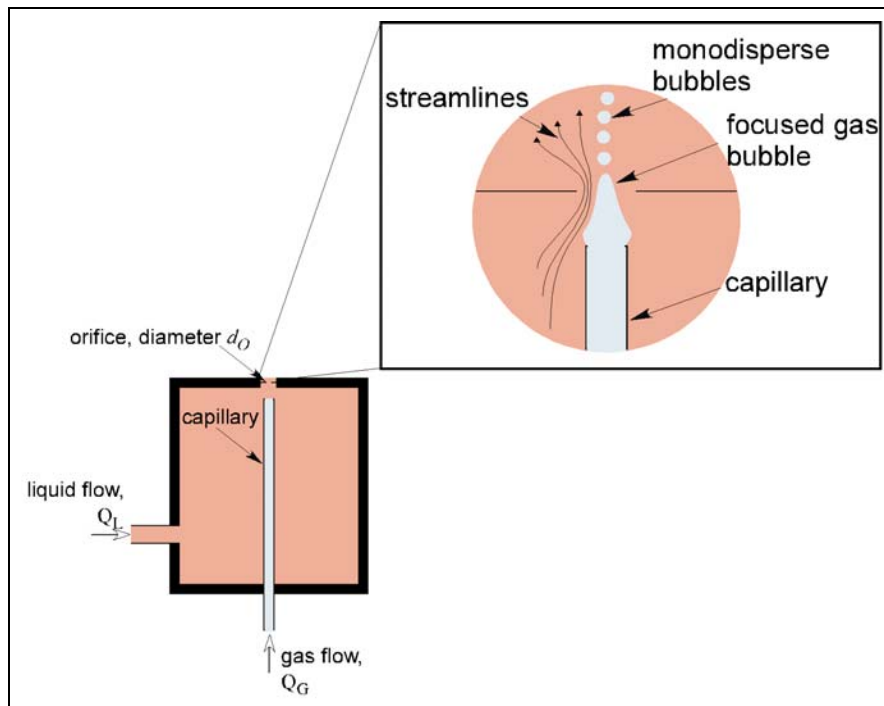


Figure 2. Schematic of bubbling device.

Bubbles are produced at remarkably fast rates with the device. The characteristic frequency of production is $\omega \sim Q_L/d_j D^2$, where Q_L is the flow rate of the liquid, d_j is the diameter of the gas jet and D is the diameter of the orifice. For typical operational parameters, the rate of production is in the kilohertz to megahertz range, which corresponds to hundreds of microliters of material produced each minute. With an array of orifices, a large amount of material could be produced very quickly.

For typical flow rates, Gañán-Calvo and Gordillo (18) found the following semiempirical relationship for bubble diameter d_b , orifice diameter d_o , gas flow rate Q_g , and liquid flow rate Q_l :

$$\frac{d_b}{d_o} = \left(\frac{Q_g}{Q_l} \right)^{0.37}. \quad (1)$$

In an analysis of steady bubbling, the important dimensionless parameter is the Weber number, which describes the relative importance of the ratio of inertia and surface tension. The Weber number (We) is defined as the following:

$$We = \frac{\rho_l v_l^2 d_j}{\gamma}, \quad (2)$$

where ρ_l , v_l , γ , and d_j are the liquid's density, velocity at the orifice, liquid-gas surface tension, and jet diameter, respectively. Gañán-Calvo found that stable, monodisperse bubbling can be achieved for $1 \leq We \leq 40$ (18). Using this criterion, it is possible to calculate the range of liquid flow rates for stable bubbling at a given orifice size. Figure 3 shows the liquid flow rate for $We = 1$ and $We = 40$, assuming that the diameter of the jet is 1/6th the diameter of the orifice. As figure 3 shows, the range of acceptable flow rates gets smaller as orifice size decreases. This means that very precise control of the flow rate is important when producing small bubbles.

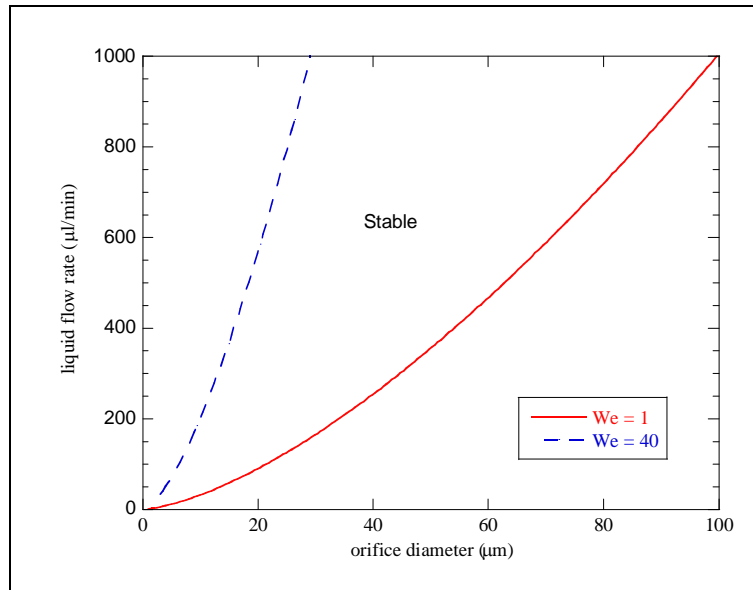


Figure 3. Liquid flow rate as a function of orifice diameter at limiting Weber numbers for stable bubbling.

The bubbling device (figure 4) consists of an aluminum cylinder with a hole bored down the center. The hole is threaded on each end to accommodate the orifice and the fittings for the gas capillary. Another threaded hole was drilled perpendicular to and through the center axis to provide a connection for the liquid. The orifice, a standard part (Lenox Laser Inc., Glen Arm, MD), is machined into the center of a standard 1/4–28 set screw. This configuration allows for easy adjustment of the distance between the capillary exit and the orifice, as well as easy removal for cleaning or a change in orifice size. Orifice diameters of 35, 50, 75, and 100 μm were used in the experiments.

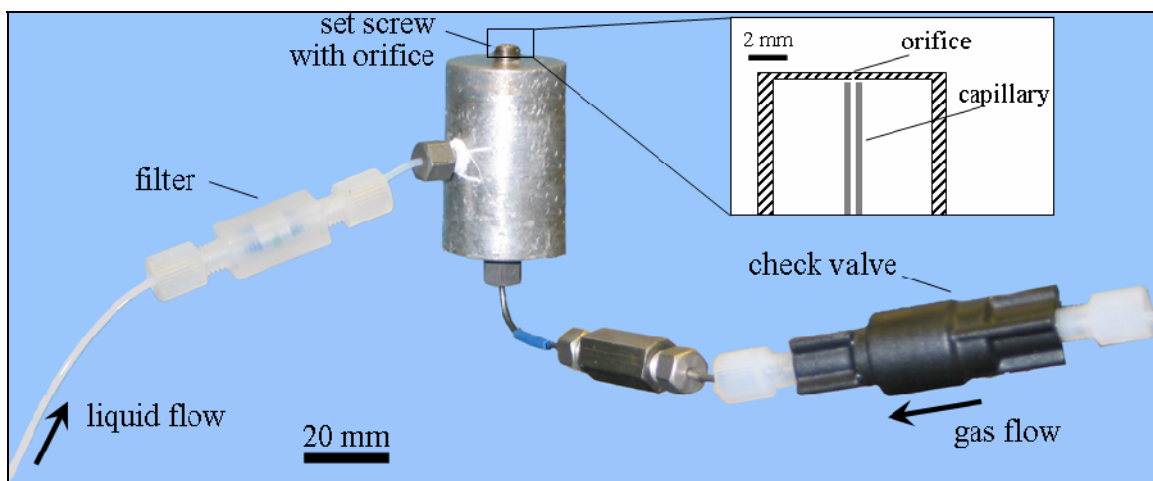


Figure 4. Bubbler with connected tubing and fittings.

The fittings and capillary (1/16-in outside diameter, 0.01-in inside diameter) are stainless steel high-performance liquid chromatography (HPLC) fittings and tubing (Upchurch Scientific, Oak Harbor, WA). An in-line filter (model A-415, Upchurch Scientific) was installed in the fluid line, and a check valve (model CV-3000NF, Upchurch Scientific) was installed in the gas line. While operation is possible without the check valve and filter, it becomes more problematic with a debris-clogged orifice and a backflow of liquid down the gas line.

The fluid and the gas flows were driven by two syringe pumps (models 22 and PHD 2000, Harvard Apparatus, Holliston, MA). Typically, the flow rate for the liquid was set between 1000 and 10 $\mu\text{L}/\text{min}$. The gas syringe pump was driven at similar speeds. However, because of compressibility, the actual flow rate is a function of other variable such as orifice size, pressure drop, and liquid surface tension.

To operate the device, the liquid line was slowly filled with solution ($\sim 50 \mu\text{L}/\text{min}$) until fluid could be seen emerging from the orifice. Then, additional fluid was added directly into the reservoir so that the fluid height was $\sim 0.5 \text{ cm}$ above the orifice. This procedure is necessary to prevent air bubbles from filling the fluid line and causing a disruption in the fluid flow and momentary polydispersity.

2.2 Materials and Procedure

2.2.1 Aqueous Foams

In order to test the device and to understand better the limits of operation, soap-water solutions were used. The solutions result in foams that are simple to make, easy to clean up, and are stable for several minutes or more.

The ease with which bubbles can be produced was studied with a 100- μm orifice. As mentioned earlier, the bubble size can be controlled by either changing the size of the orifice or changing the relative flow rate of the liquid and gas. Gañán-Calvo and Gordillo found a power-law relationship between the relative flow rate and bubble size with an exponent of 0.37. In order to study this behavior, the bubbles were produced with various flow rates and using orifices of various sizes.

The bubble solution was 40 parts water, 10 parts glycerin, and 1 part sodium dodecyl sulfate (SDS). Filtered water (HPLC Water, 0.2-mm filter, J. T. Baker, Phillipsburg, NJ) was used to keep the orifice from clogging. The glycerin serves to slow down the evaporation of the water, which can speed up bubble rupture. SDS (Sigma-Aldrich, St. Louis, MO) is a surfactant for stabilizing the bubble films. The bubble recipe used in this work is not necessarily the optimum one.

2.2.2 Solid Foams

As previously discussed, the material used to manufacture photonic crystals should have a high refractive index, and the liquid precursor should have a fairly low viscosity so it can readily be pumped through the bubbler apparatus. Most importantly, the precursor should support a stable foam so the crystal structure can be maintained throughout solidification. The first attempts at producing a solid, ordered foam were made using polymers. These polymer foams were used as templates to produce ceramic foams.

2.2.2.1 Polymer Foams

Initial efforts to produce solid, ordered foams using epoxy and UV-cured urethane were unsuccessful, since these materials could not produce a foam stable enough to preserve ordering through solidification. Instead, we manufactured the foam using aqueous solutions of hydrogel monomers. Since surfactants are most active in polar liquids, water is an excellent medium for producing stable foams.

We used an acrylamide monomer (Sigma-Aldrich, St. Louis, MO), with methylene bis-acrylamide (Sigma-Aldrich, St. Louis, MO) as the crosslinker. In addition, methylcellulose (Methocel A15LV Dow Chemical, Midland, MI) was used to aid in bubble stabilization. The bubbling solution was made by first preparing a 1% dispersion of Methocel in HPLC-grade water, according to the manufacturer's recommendation. Then, 180 parts of the water solution

were mixed with 60 parts acrylamide, 3 parts methylene bis-acrylamide, and 1 part SDS (by weight). Ammonium persulfate (Sigma-Aldrich, 30% in water, by weight) was used as the initiator with tetraethylmethylenediamine (TEMED) (Sigma-Aldrich, 20% in water, by weight) as the catalyst.

Since the free radical polymerization of acrylamide is inhibited by oxygen, the syringes were purged with nitrogen before bubbling. Then, as with the aqueous solutions, the liquid line was slowly filled with solution ($\sim 50 \mu\text{L}/\text{min}$) until fluid could be seen emerging from the orifice. Then, additional fluid was added directly to the orifice so that the fluid height was $\sim 0.5 \text{ cm}$ above the orifice.

Two techniques were used to solidify the aqueous polymer foam. In technique no. 1, a drop of initiator was added to the reservoir just as the white plume of bubbles was observed issuing from the orifice. Without a catalyst, the reaction incubation time is long enough for bubbling to continue for several minutes without clogging the system with polymer. After enough foam had been generated, a portion of the foam was scooped into a small vial. Finally, a drop of TEMED solution was placed into the vial, and the sample was left to polymerize under flowing nitrogen.

Technique no. 2 was developed in order to manufacture higher quality specimens. As in technique no. 1, a drop of initiator was added to the reservoir just after bubbling commenced. After enough foam had been generated, a portion was placed on a clean glass slide under a source of flowing nitrogen. Another glass slide was covered with TEMED solution and placed on top of the foam. As shown in figure 5, spacers were used to separate the two slides. The sample was left to polymerize for about 10 min before handling.

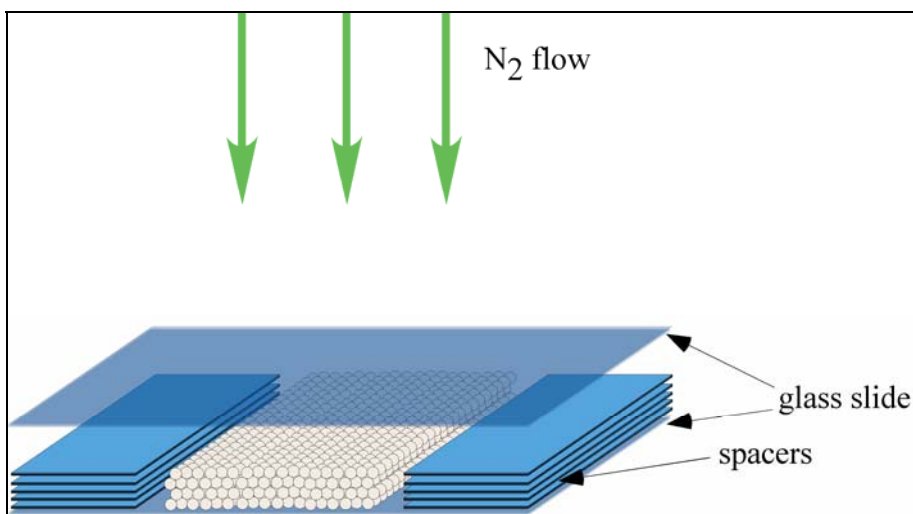


Figure 5. Schematic of technique for producing solid acrylamide foams.

2.2.2.2 Ceramic Foams

The techniques described in the previous section demonstrate that the bubbling device can be used to produce permanent, ordered polymeric foams. However, as mentioned earlier, ceramic foams are preferred because optical performance increases with the index contrast between the PBGM's high and low index phases.

Monodisperse ceramic foam is produced from the acrylamide foams already described. With this technique, the polymer foam (discussed in section 2.2.2.1) is used as a template for the ceramic foam. Since acrylamide is water soluble, a water-based ceramic precursor was used to infiltrate the hydrogel foam and replace the water in the walls of the foam with the ceramic precursor. The precursor was a solution of 4 parts ethanol, 6 parts TEOS (Sigma-Aldrich, St. Louis, MO), and 3 parts deionized water with the pH adjusted, using hydrochloric, to ~1, and the template was soaked in the solution for 1–2 days. After the ceramic gelled at room temperature, the material was heated at 10 °C/min to 550 °C for 2 hr to burn off the polymer and strengthen the ceramic.

2.2.3 Emulsions

In addition to producing liquid and solid foams, the bubbling device was also used to produce monodisperse oil-in-water emulsions. The emulsions were produced by replacing the gas in the aqueous foam experiments previously described with octane (Sigma-Aldrich, St. Louis, MO). The orifice size was 100 μm , and the flow rates for the water and oil were ~400 and 100 $\mu\text{L}/\text{min}$, respectively.

3. Results and Discussion

3.1 Aqueous Foams

When bubbling commences, the bubbles emerge from the orifice in a fountain at a very high rate of production (approximately kilohertz to megahertz). Viewed with the naked eye, the fountain appears as a white plume. Since each bubble resonates as it is formed, a continuous high-pitched monotone whine can be heard when the bubbles are monodisperse. Figure 6 shows a magnified top view of the bubbler in operation. Once formed, the bubbles are pulled into a hexagonal lattice by surface tension.

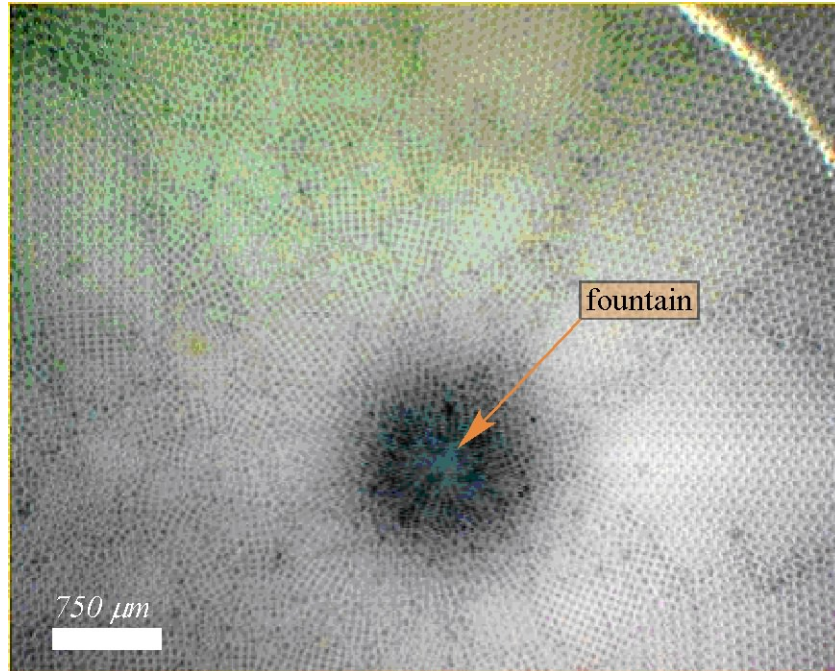


Figure 6. View of bubble fountain from above (75- μm orifice).

Figures 7–10 show additional images of bubble crystals produced with orifices from 35 to 100 μm at various flow rates. In all cases, the bubbles' monodispersity is apparent by their packing into regular lattices, dozens of repeat units across. Braun and Wiltzius (30) mention that particles must be monodisperse to within 5% to obtain good ordering, while Jiang et al. (31) show very good and very poor ordering for particles with size standard deviations of 3.8% and 14.2%, respectively. While hexagonal packing is by far the more prevalent, a few grains show apparent cubic packing in the top surface of the foam. These cubic crystals appear to be more prominent near the fountain, where the crystals have more energy and perhaps have not had time to relax to the more efficient hexagonal packing. Figure 9 shows evidence that packing extends to the second layer of bubbles and figure 11 shows packing down to the third layer. The appendix contains additional images of bubble crystals.

Figure 12 shows the results of various flow rates. As expected, the bubble size can be controlled by varying the relative flow rate, and the behavior is power-law in the relative flow rate. However, the bubble size is not as sensitive to relative flow rate as reported by Gañán-Calvo and Gordillo (18) with an exponent of 0.37 (compared to 0.27 in the present work). Furthermore, the exponent of the power-law behavior reported by Gañán-Calvo and Gordillo (one), indicates that for a relative flow rate of one, the bubble diameter equals the orifice diameter. The bubbles produced in this study resulted in an exponent of 1.34, which means that for relative flow rate equal to one, the bubble is 34% larger than the orifice diameter.

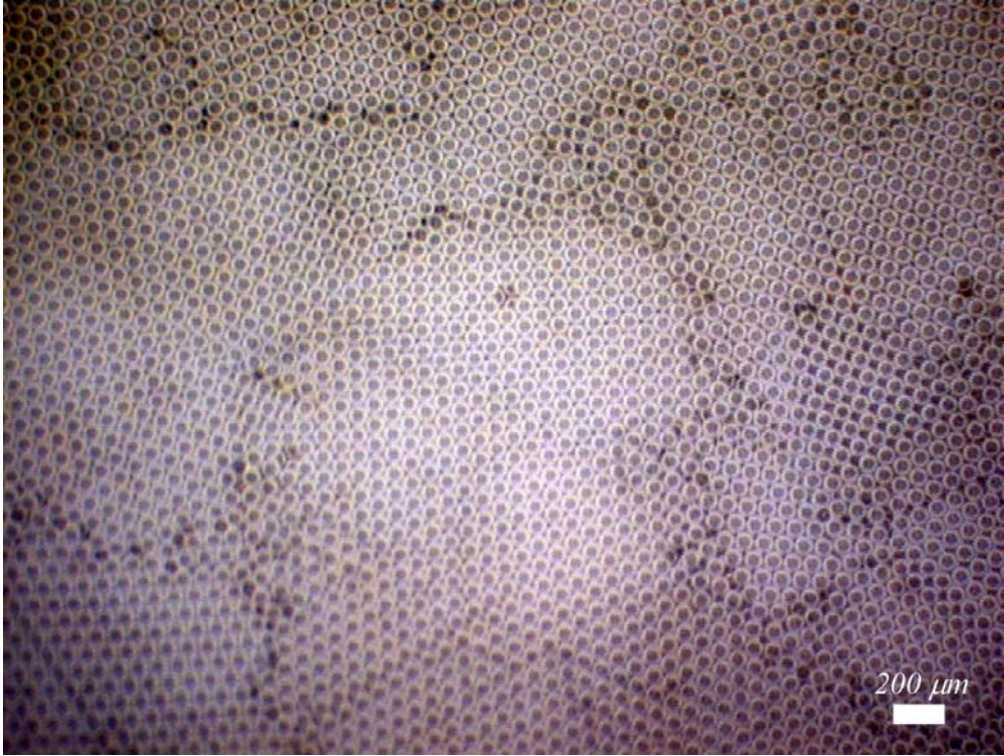


Figure 7. Bubbles produced with 50- μm orifice ($Q_l = Q_g = 250 \mu\text{L}/\text{min}$).

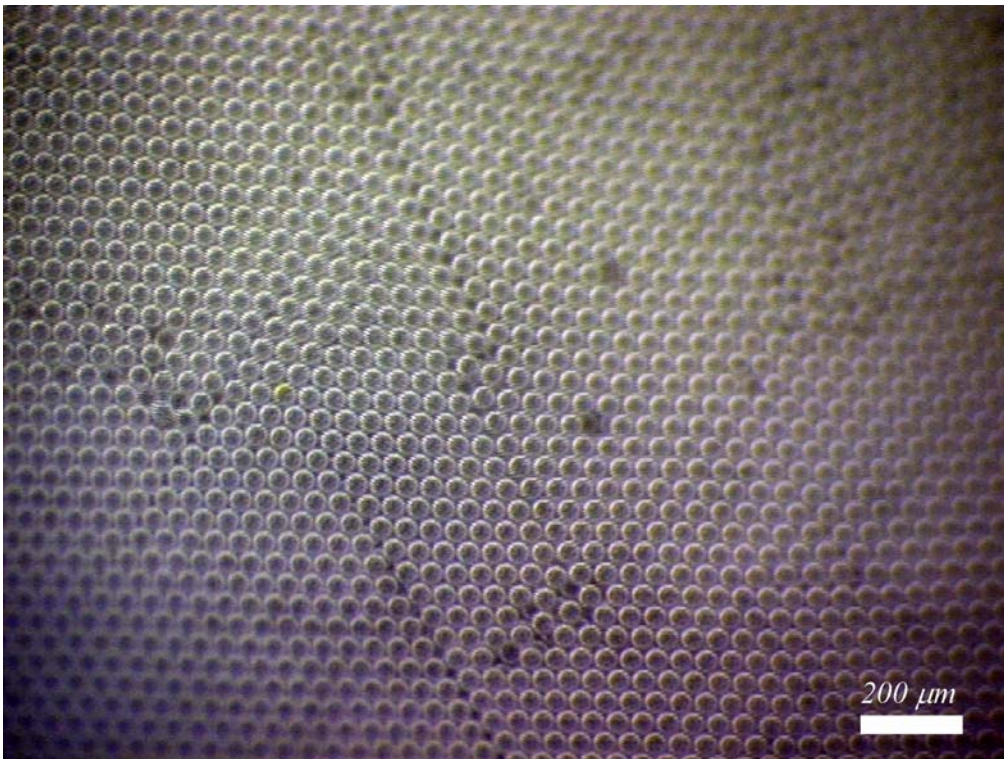


Figure 8. Bubbles produced with 35- μm orifice ($Q_l = 64 \mu\text{L}/\text{min}$, $Q_g = 32 \mu\text{L}/\text{min}$).

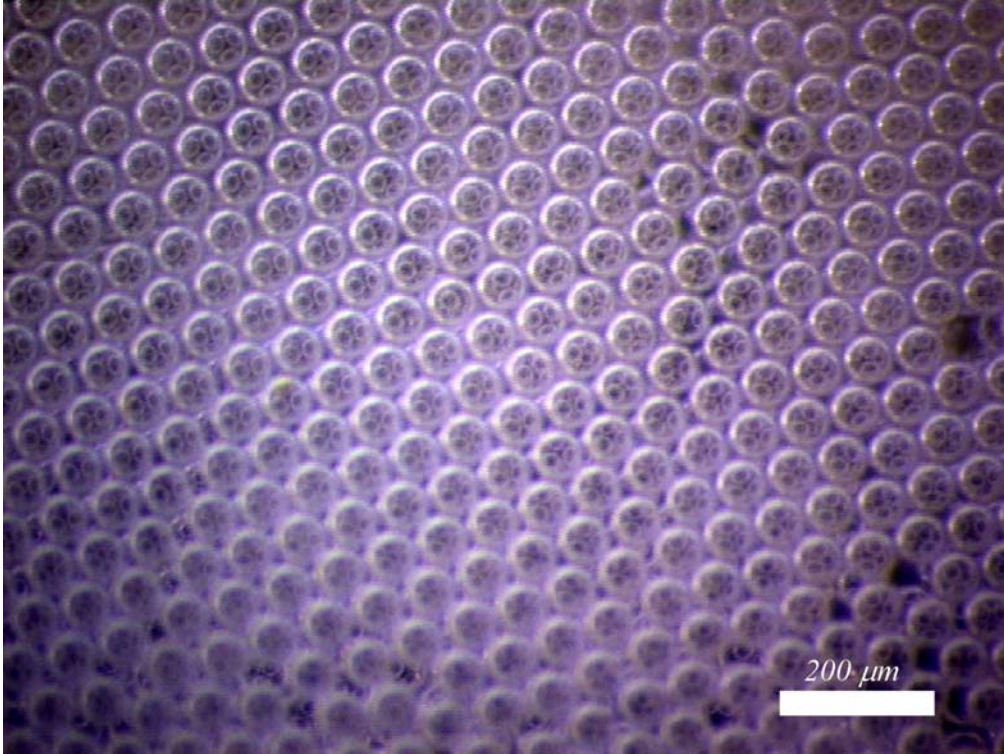


Figure 9. Bubbles produced with 35- μm orifice ($Q_l = Q_g = 64 \mu\text{L}/\text{min}$).

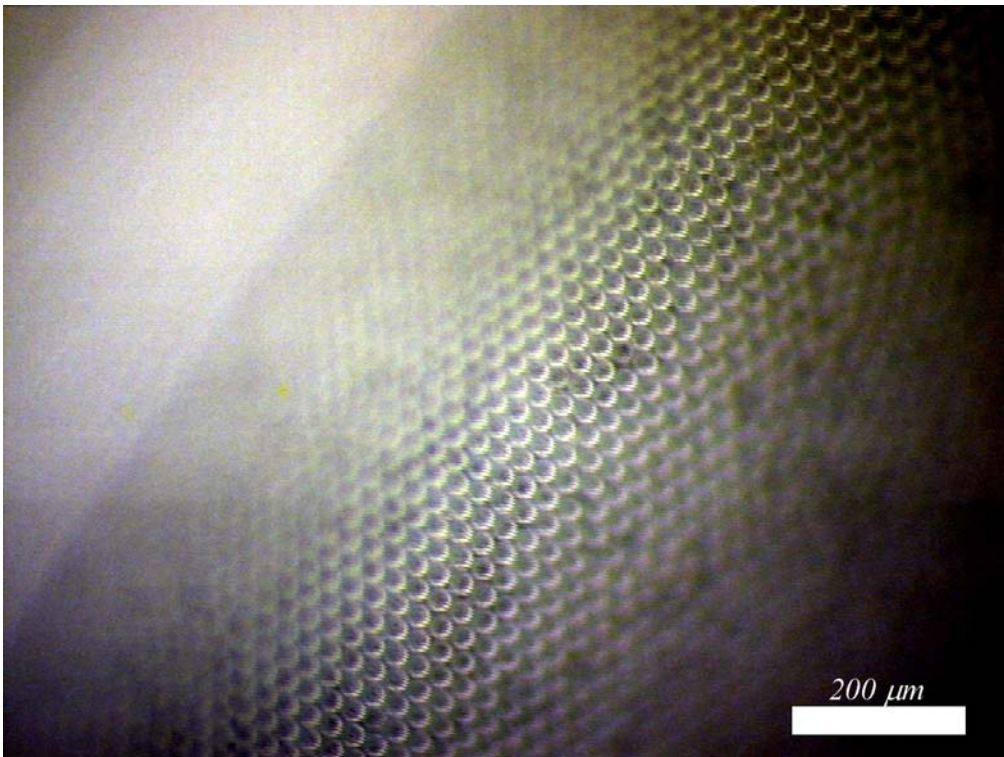


Figure 10. Bubbles produced with 35- μm orifice ($Q_l = 64 \mu\text{L}/\text{min}$, $Q_g = 8 \mu\text{L}/\text{min}$).

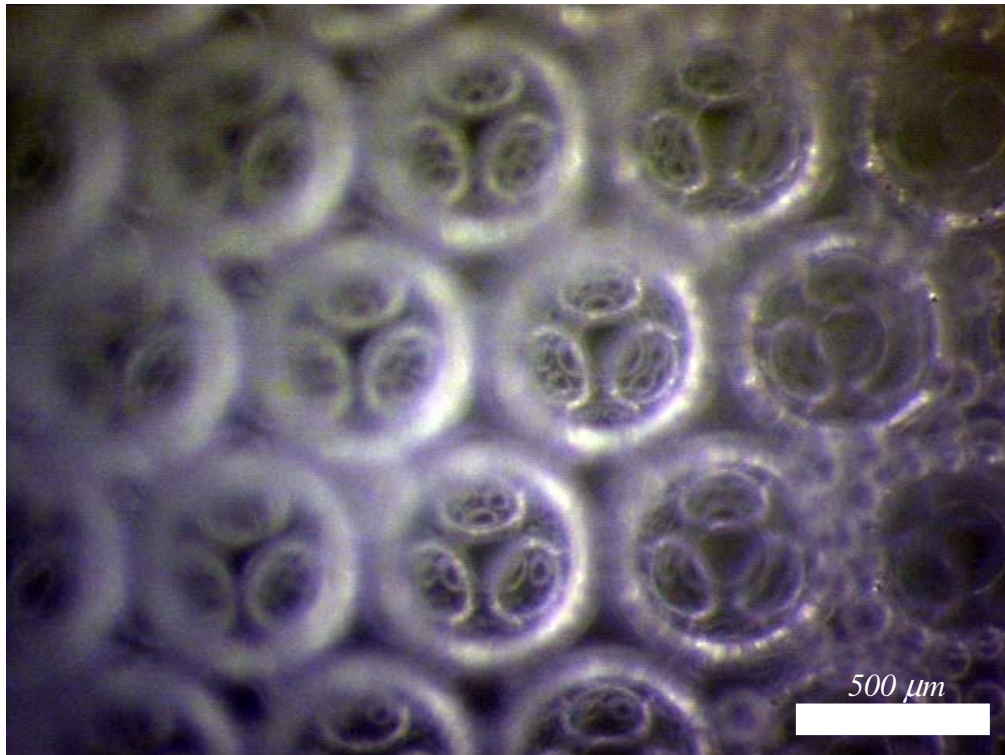


Figure 11. Evidence of ordering through three bubble layers. Scale unknown.

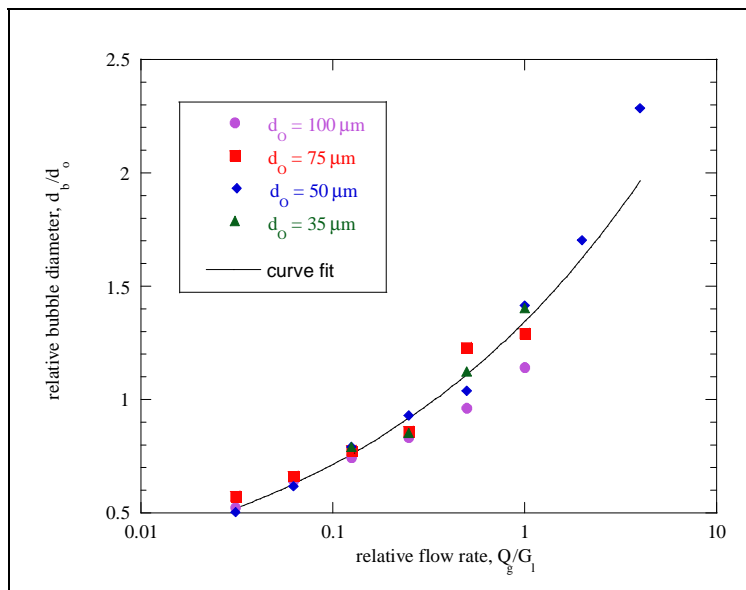


Figure 12. Bubble size control through relative flow rate.

There are many possible explanations for this inconsistency. As an example, the flow rates in this study were fairly narrow. Perhaps if a wider range were considered, as Gañán-Calvo and Gordillo did, the exponent would change. However, the inconsistency is most likely because of differences in details, such as the orifice and capillary geometry used in each work. These differences likely resulted in different pressure drops across the orifice for a given gas flow rate specified at the syringe pump.

The smallest bubbles produced were $\sim 25 \mu\text{m}$. These bubbles, obtained using a 35-mm orifice, are shown in figure 10. While the relative flow rate can be manipulated to reduce bubble size, it becomes impractical to use a liquid flow rate greater than about $20\times$ the gas flow rate.

Therefore, as demonstrated by equation 1, the bubbles cannot be reduced much below a third of the orifice diameter, and in order to decrease bubble size, smaller and smaller orifices must be used. Unfortunately, obtaining stable bubbling became increasingly difficult as the orifice size decreased, and it could not be achieved using orifices below $35 \mu\text{m}$. This is likely a result of the specifics of the orifice geometry. All orifices used in this study, regardless of diameter, were manufactured in stainless steel of the same thickness, $250 \mu\text{m}$. For the larger diameter holes, this thickness is small enough for the hole to be considered an orifice. In the ideal, thin-orifice case, the gas ligament extends only a small distance from the exit of the orifice before the capillary instability breaks the ligament into a bubble. If the orifice or hole is too long, then the instability will occur inside the hole, will likely be subject to perturbations there, and will make stable bubbling difficult to achieve.

3.2 Solid Foam

3.2.1 Polymer

Figure 13 shows an acrylamide sample after processing with technique no. 1. The sample has several regions of ordered foam. However, the ordering is not preserved over much of the sample.

Polymerizing the sample between glass slides (technique no. 2) resulted in much better specimens with preserved ordering over much larger regions. The method used for introducing the accelerator (TEMED) in technique no. 2 results in a more even distribution of the chemical and a more uniform polymerization that better preserves the structure. Figures 14 and 15 show two magnifications of a sample manufactured in this manner. The lower magnification image shows fairly large grains of ordered bubbles, and the higher magnification image shows ordering in the second layer of the structures. Figures 16 and 17 show images of another sample taken with the microscope focused on the first and second layers, respectively.

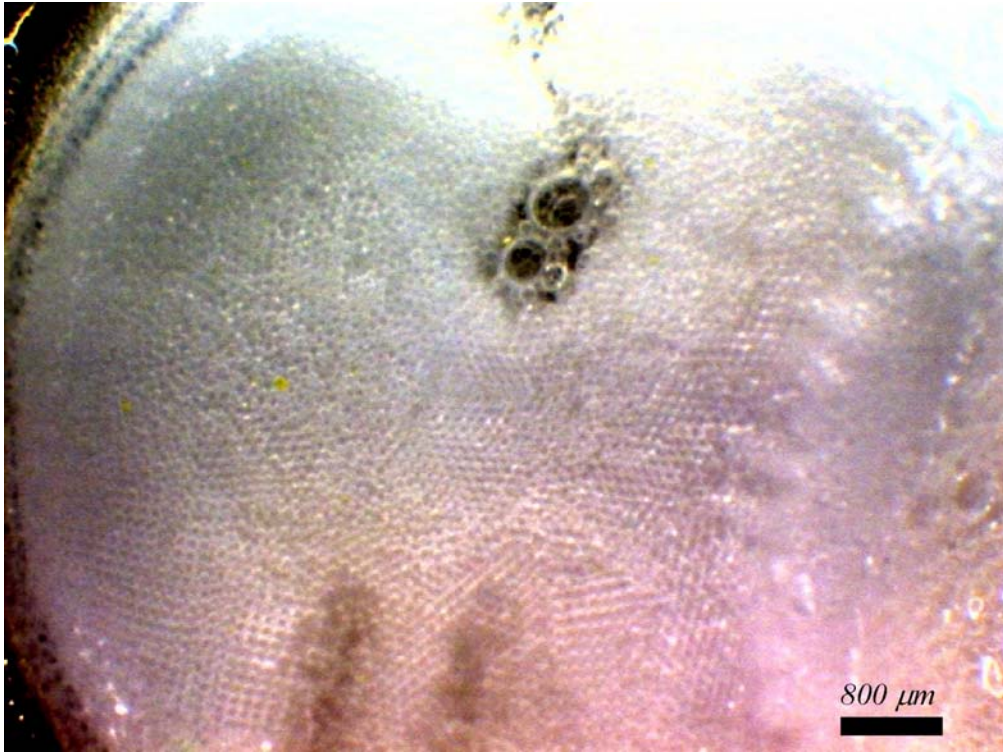


Figure 13. Acrylamide monodisperse polymeric foam after processing with technique no. 1.

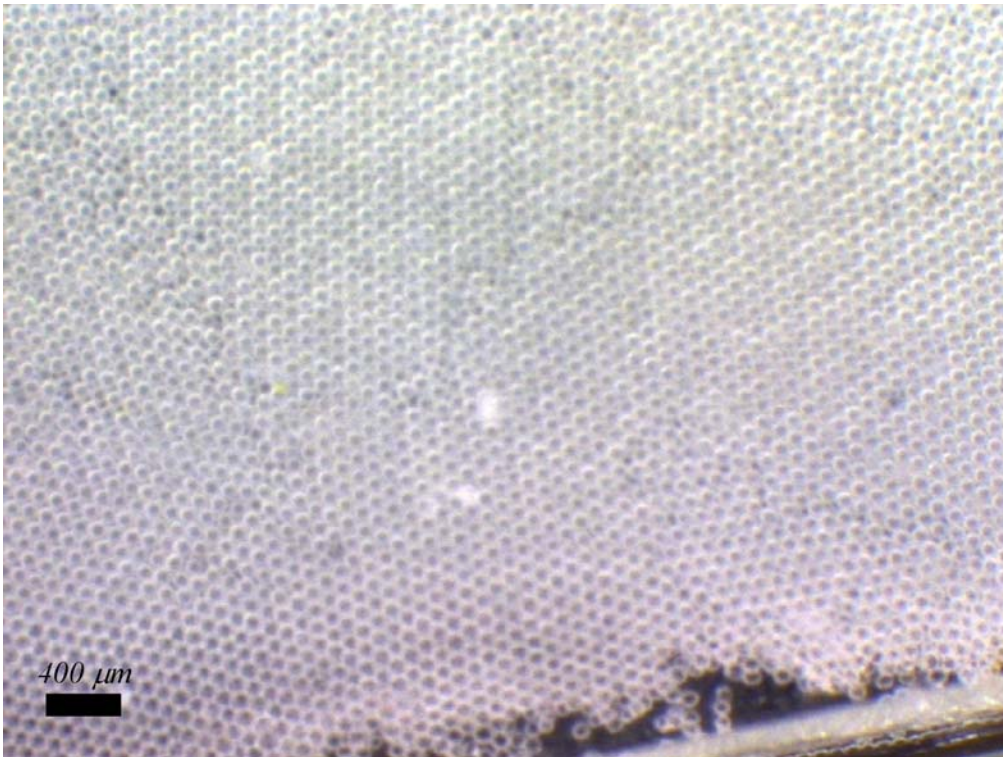


Figure 14. Acrylamide monodisperse polymeric foam after processing with technique no. 2 (lower magnification).

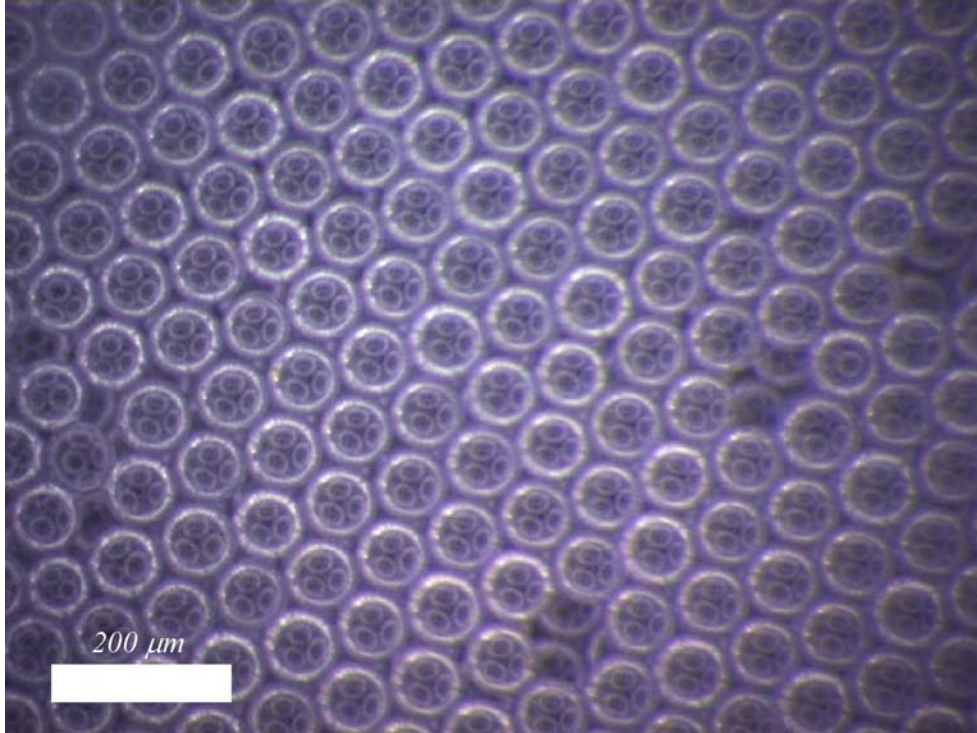


Figure 15. Acrylamide monodisperse polymeric foam after processing with technique no. 2 (higher magnification).

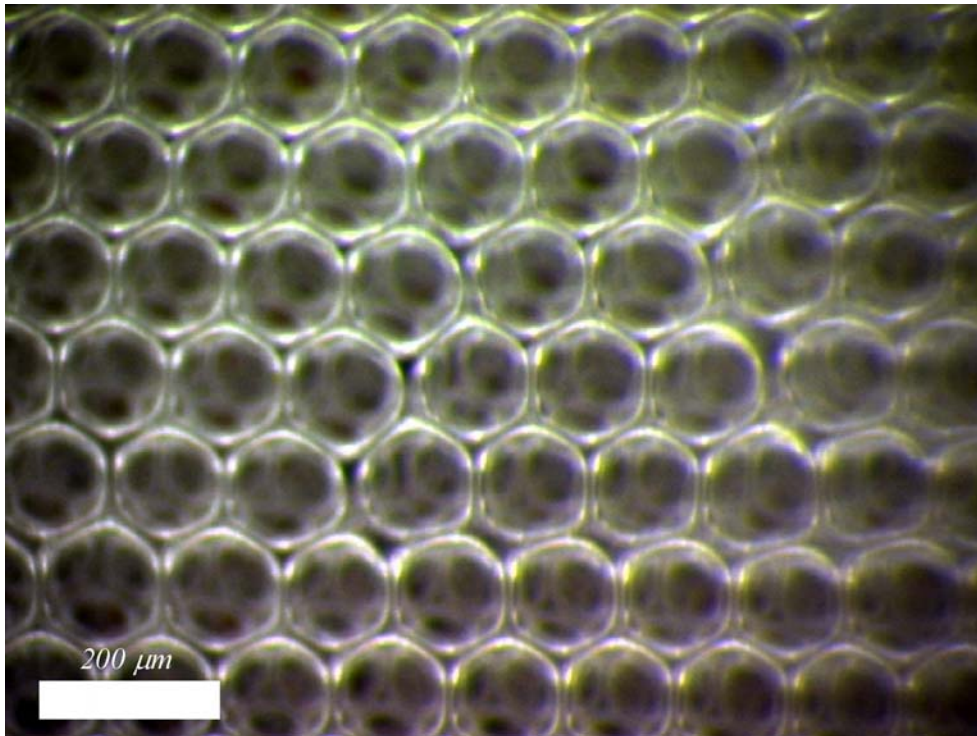


Figure 16. Acrylamide foam. Micrograph taken with microscope focused on the first layer of bubbles, nearest the camera.

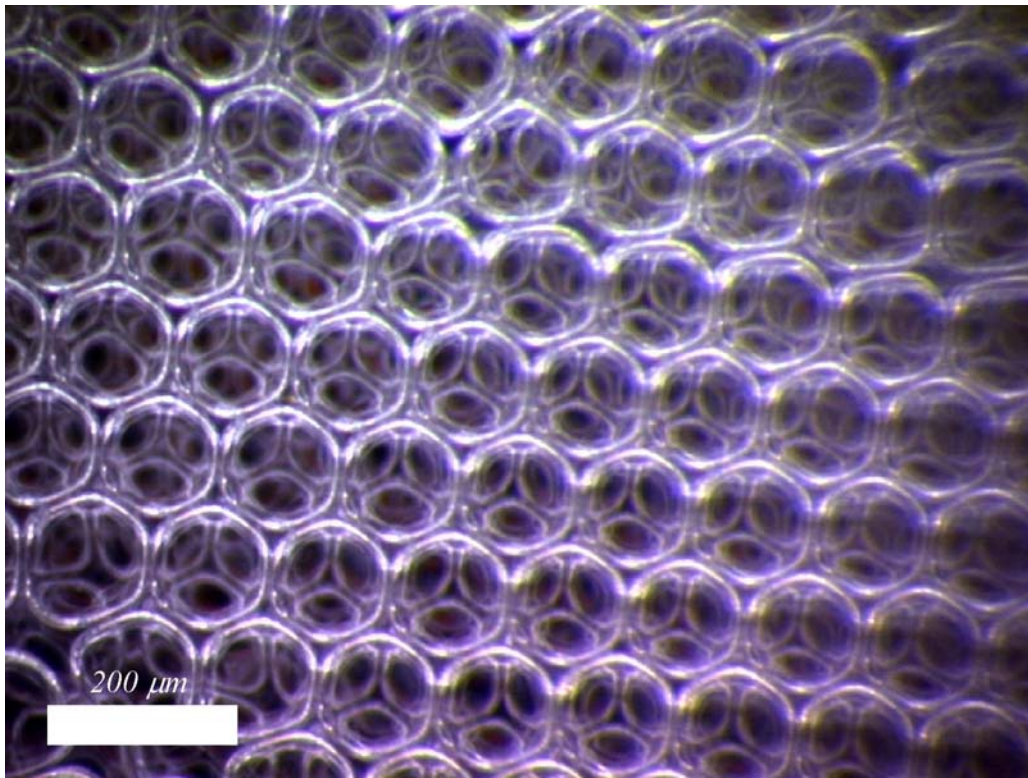


Figure 17. Acrylamide foam. Micrograph taken with microscope focused on the second layer of bubbles.

3.2.2 Ceramic

Figures 18 and 19 show results of silica foams produced from acrylamide templates. The templates used in these trials were ordered in only a few small regions. However, as the figures show, the structure of the hydrogel foam, including the ordered regions, was preserved. Macroscopically, the ceramic foams exhibit significant warpage from drying, and they are quite fragile.

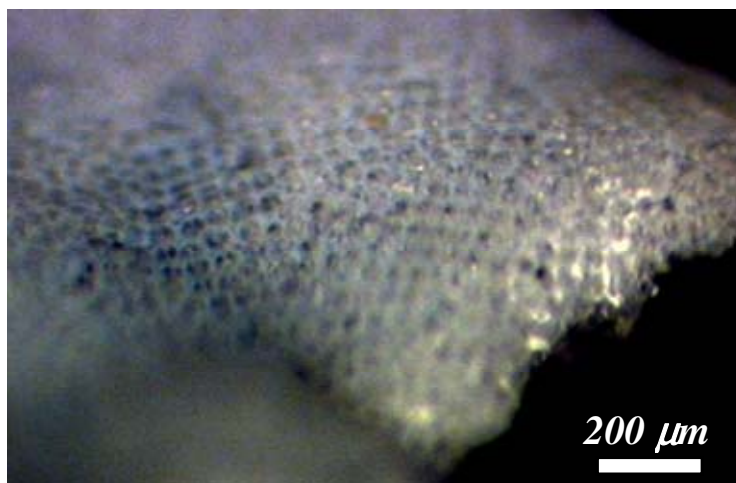


Figure 18. Silica gel produced from acrylamide template (sample 1).

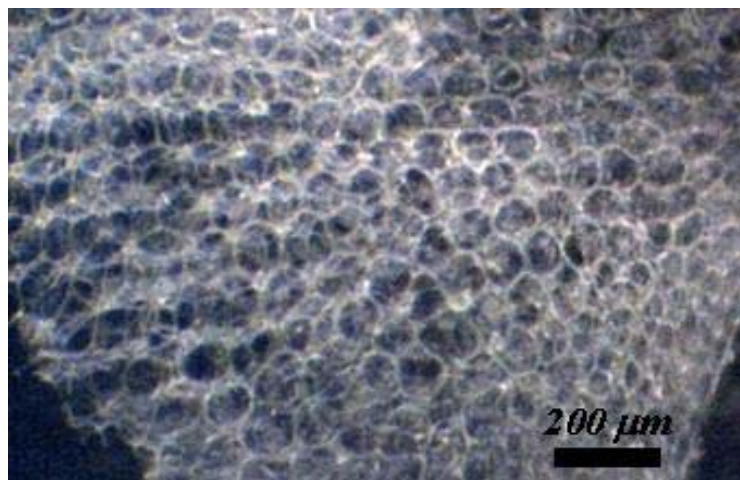


Figure 19. Silica gel produced from acrylamide template (sample 2).

3.3 Emulsions

As mentioned earlier, the bubbling device outlined in this report (and previously by Gañán-Calvo and Gordillo [18]) can be used to produce monodisperse emulsions. Figure 20 shows a monodisperse emulsion produced using the bubbler with a 100- μm orifice. As with the bubbles in the monodisperse foams, the oil droplets readily arrange themselves in a close-packed array.

If methods for directly producing high-quality monodisperse ceramic foam with bubbling are not successful, monodisperse emulsions could be used as templates to produce PBGMs. This technique, developed by Imhof and Pine (11), involves making a monodisperse emulsion with a ceramic precursor as the continuous phase. The emulsion technique could produce superior-quality foams, since the oil droplets would constrain the matrix from deforming during solidification much better than the air droplets of the bubbling technique. In the past, the emulsion-templating method has been limited by the tedious fractionation process that is necessary to produce the monodisperse emulsion.

4. Summary and Conclusions

A technique for the low-cost production of periodic structures has been developed using a capillary flow focusing device that produces monodisperse foams and emulsions. The technique is easily scalable (since the device can produce bubbles at a very high rate), is simple to construct, and a large array of bubblers could be used to produce a large quantity of foam in a short amount of time. Also, the technique allows for a wide range of feature sizes and can be extended to polymeric and ceramic materials.

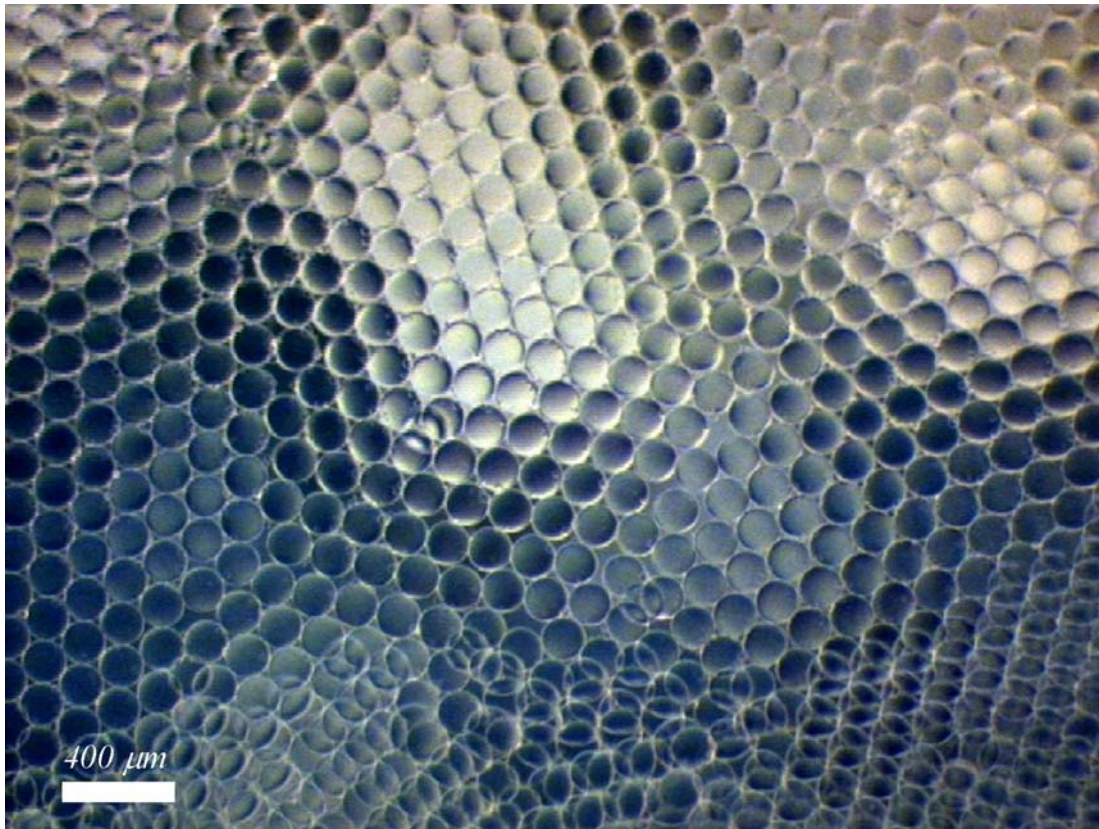


Figure 20. Ordering of monodisperse water-octane emulsion stabilized with SDS.

Although the viability of producing ordered foams through bubbling has been demonstrated in this report, there are many avenues that should be pursued to improve the technique. Perhaps the most important area for improvement is the bubble size. For PBGMs to be useful, the feature size should be, at most, $10\ \mu\text{m}$. As previously mentioned, bubbles smaller than about $25\ \mu\text{m}$ have not been produced in this work, a limitation that could result from the severe aspect ratios of the smaller orifices. However, efforts focused on the design and testing of a bubbler device that does not suffer from such severe aspect ratios at small diameters has not yielded noticeably smaller bubbles. Alternatively, the minimum bubble size could be limited by physics. Since the internal bubble pressure is inversely proportional to diameter, gas more readily diffuses out of the bubble with decreasing diameter, which further decreases the diameter and raises the pressure until the bubble collapses on itself. If the minimum bubble size does prove to be too large for PBGM applications, the bubbling device can be used to make monodisperse liquid-liquid emulsions that would not suffer from the same size limitations as monodisperse foams.

Once crystals of smaller bubbles can be manufactured, the optical properties of the PBGMs can be investigated using an infrared microscope. The microscope could also be used along with the bubbler to measure optical properties during bubbling. This technique would provide a direct measure of the PBGM's optical properties as a function of the number of repeat units through the thickness of the crystal.

Efforts should also be undertaken to improve the quality of the solid foam crystals. The difference in acrylamide foams produced by technique nos. 1 and 2 demonstrated that the processing method used for solidifying the foam is critical to the quality of the final product. Better crystals could be produced by incorporating a UV initiator into the polymer solution used for bubbling. Unfortunately, the UV initiators tried so far have been incompatible with the foam, acting as “defoamers.” Improving the crystals’ quality will probably improve the PBGM’s response in both magnitude and predictability. Better crystals could be achieved through a shear annealing technique similar to Xu et al. (5). Or, the crystals could be annealed by raising the mechanical temperature through low amplitude oscillations provided by a shaker. This technique is similar to annealing in metals, where the material is raised to a temperature a couple of hundred degrees below its melting temperature. The elevated temperature gives the atoms enough mobility to increase grain size and decrease the overall energy of the system. Another path to improved crystals is through the elimination of stacking faults by epitaxial growth from a patterned template (32).

It also may be possible to tailor the optical properties of the material by using more complicated geometries than the monodisperse configurations described so far. For example, using the technique in this report, it would be easy to dynamically control the bubble size. This could result in a periodic structure with bi-disperse features or a gradient in feature size. Feedback of bubble size during dynamic variation could be provided by the acoustic measurements (33).

Other improvements to the process will be realized by searching for better, more efficient pathways to the production of high index contrast ceramic PBGMs. There are undoubtedly many ways to accomplish this. For example, better surfactants and other stabilization methods could be used to better preserve the as-bubbled crystal structure during bubbling. This might include using polymerizable surfactants (surfamers), which would provide additional support to the thin bubble walls. Also, nanoparticles functionalized with surfactants could be used to load the bubble walls with higher index material and to reduce the shrinkage during conversion of the hydrogel to ceramic. Additionally, the process could be made much more efficient by bubbling directly into a ceramic precursor solution. This would be accomplished with the right choice of precursor and foam stabilizers so that the material gels before the foam is destroyed. Finally, any improvement to the technique should include the incorporation of high index ceramics such as chalcogenides, a family of sulfur, selenium, or tellurium-containing ceramics, which will assist in better PBGM performance.

5. References

1. Joannopoulos, J. D.; Meade, R. D.; Winn, J. N. *Photonic Crystals – Molding the Flow of Light*; Princeton University Press: Princeton, NJ, 1995.
2. Parker, G.; Charlton, M. Photonic Crystals, in Physics Web. www.physicsweb.org (accessed 1 August 2000).
3. Pralle, M. U.; Moelders, N.; McNeal, M. P.; Puscasu, I.; Greenwald, A. C.; Daly, J. T.; Johnson, E. A.; George, T.; Choi, D. S.; El-Kady, I.; Biswas, R. Photonic Crystal Enhanced Narrow-Band Infrared Emitters. *Applied Physics Letters* **2002**, *81* (25), 4685–4687.
4. Schroden, R. C.; Al-Daous, M.; Blanford, C. F.; Stein, A. Optical Properties of Inverse Opal Photonic Crystals. *Chemistry of Materials* **2002**, *14* (8), 3305–3315.
5. Xu, Y.; Schneider, G. J.; Wetzel, E. D.; Prather, D. W. Centrifugation and Spin-Coating Method for Fabrication of Three-Dimensional Opal and Inverse-Opal Structures As Photonic Crystal Devices. *Journal of Microlithography Microfabrication and Microsystems* **2004**, *3* (1), 168–173.
6. Gates, B.; Yin, Y. D.; Xia, Y. N. Fabrication and Characterization of Porous Membranes With Highly Ordered Three-Dimensional Periodic Structures. *Chemistry of Materials* **1999**, *11* (10), 2827–2836.
7. Srinivasarao, M.; Collings, D.; Philips, A.; Patel, S. Three-Dimensionally Ordered Array of Air Bubbles in a Polymer Film. *Science* **2001**, *292* (5514), 79–83.
8. Sharp, D. N.; Turberfield, A. J.; Campbell, M.; Denning, R. G. Photonic Crystals for the Visible Spectrum by Holographic Lithography. *Optical and Quantum Electronics* **2002**, *34* (1–3), 3–12.
9. Kondo, T.; Matsuo, S.; Juodkazis, S.; Misawa, H. Femtosecond Laser Interference Technique With Diffractive Beam Splitter for Fabrication of Three-Dimensional Photonic Crystals. *Applied Physics Letters* **2001**, *79* (6), 725–727.
10. Fink, Y.; Urbas, A. M.; Bawendi, M. G.; Joannopoulos, J. D.; Thomas, E. L. Block Copolymers as Photonic Bandgap Materials. *Journal of Lightwave Technology* **1999**, *17* (11), 1963–1969.
11. Imhof, A.; Pine, D. J. Ordered Macroporous Materials by Emulsion Templating. *Nature* **1997**, *389* (6654), 948–951.
12. Ruhl, T.; Spahn, P.; Hellmann, G. P. Artificial Opals Prepared by Melt Compression. *Polymer* **2003**, *44* (25), 7625–7634.

13. Tuncel, A.; Kahraman, R.; Piskin, E. Monosize Polystyrene Microbeads by Dispersion Polymerization. *Journal of Applied Polymer Science* **1993**, *50* (2), 303–319.
14. Imhof, A.; Pine, D. J. Uniform Macroporous Ceramics and Plastics by Emulsion Templating. *Advanced Materials* **1998**, *10* (9), 697–700.
15. Shafi, M. A.; Joshi, K.; Flumerfelt, R. W. Bubble Size Distributions in Freely Expanded Polymer Foams. *Chemical Engineering Science* **1997**, *52* (4), 635–644.
16. Lin, J. N.; Banerji, S. K.; Yasuda, H. Role of Interfacial-Tension in the Formation and the Detachment of Air Bubbles 1. A Single Hole on a Horizontal Plane Immersed in Water. *Langmuir* **1994**, *10* (3), 936–942.
17. Lin, H. B.; Eversole, J. D.; Campillo, A. J. Vibrating Orifice Droplet Generator for Precision Optical Studies. *Review of Scientific Instruments* **1990**, *61* (3), 1018–1023.
18. Gañán-Calvo, A. M.; Gordillo, J. M. Perfectly Monodisperse Microbubbling by Capillary Flow Focusing. *Physical Review Letters* **2001**, *87* (27).
19. Gañán-Calvo, A. M. *Device and Method for Fluid Aeration via Gas Forced Through a Liquid Within an Orifice of a Pressure Chamber*. U.S. Patent 6,196,525, 6 March 2001.
20. Rosen, M. J. *Surfactant and Interfacial Phenomena*; John Wiley & Sons: New York, NY, 1978.
21. Sebba, F. *Foams and Biliquid Foams – Aphrons*; John Wiley and Sons: New York, NY, 1987.
22. Lai, K.; Dixit, N. *Additives for Foams, in Foams – Theory, Measurements, and Applications*; Prud'homme, R. K., Khan, S. A., Eds.; Marcel Dekker Inc.: New York, NY, 1996.
23. Schmidt, D. L. *Nonaqueous Foams, in Foams – Theory, Measurements, and Applications*; Prud'homme, R. K., Khan, S. A. Eds., Marcel Dekker Inc.: New York, NY, 1996.
24. The Dow Chemical Company. *Methocel Cellulose Ethers, Dow Technical Handbook*; Midland, MI, 2002.
25. Bindal, S. K.; Sethumadhavan, G.; Nikolov, A. D.; Wasan, D. T. Foaming Mechanisms in Surfactant Free Particle Suspensions. *Aiche Journal* **2002**, *48* (10), 2307–2314.
26. Gañán-Calvo, A. M.; Fernández, J. M.; Oliver, A. M.; Marquez, M. Coarsening of Monodisperse Wet Microfoams. *Applied Physics Letters* **2004**, *84* (24), 4989–4991.
27. Santos, E. P.; Santilli, C. V.; Pulcinelli, S. H. Formation of Zirconia Foams Using the Thermostimulated Sol-Gel Transition. *Journal of Non-Crystalline Solids* **2002**, *304* (1–3), 143–150.

28. Wu, M. X.; Fujii, T.; Messing, G. L. Synthesis of Cellular Inorganic Materials by Foaming Sol Gels. *Journal of Non-Crystalline Solids* **1990**, *121* (1–3), 407–412.
29. Gordillo, J. M.; Gañán-Calvo, A. M.; Perez-Saborid, M. Monodisperse Microbubbling: Absolute Instabilities in Coflowing Gas-Liquid Jets. *Physics of Fluids* **2001**, *13* (12), 3839–3842.
30. Braun, P. V.; Wiltzius, P. Macroporous Materials - Electrochemically Grown Photonic Crystals. *Current Opinion in Colloid & Interface Science* **2002**, *7* (1–2), 116–123.
31. Jiang, P.; Bertone, J. F.; Hwang, K. S.; Colvin, V. L. Single-Crystal Colloidal Multilayers of Controlled Thickness. *Chemistry of Materials* **1999**, *11* (8), 2132–2140.
32. Braun, P. V.; Zehner, R. W.; White, C. A.; Weldon, M. K.; Kloc, C.; Patel, S. S.; Wiltzius, P. Epitaxial Growth of High Dielectric Contrast Three-Dimensional Photonic Crystals. *Advanced Materials* **2001**, *13* (10), 721–724.
33. Chanson, H.; Manasseh, R. Air Entrainment Processes in a Circular Plunging Jet: Void-Fraction and Acoustic Measurements. *Journal of Fluids Engineering-Transactions of the ASME* **2003**, *125* (5), 910–921.

INTENTIONALLY LEFT BLANK.

Appendix. Additional Images

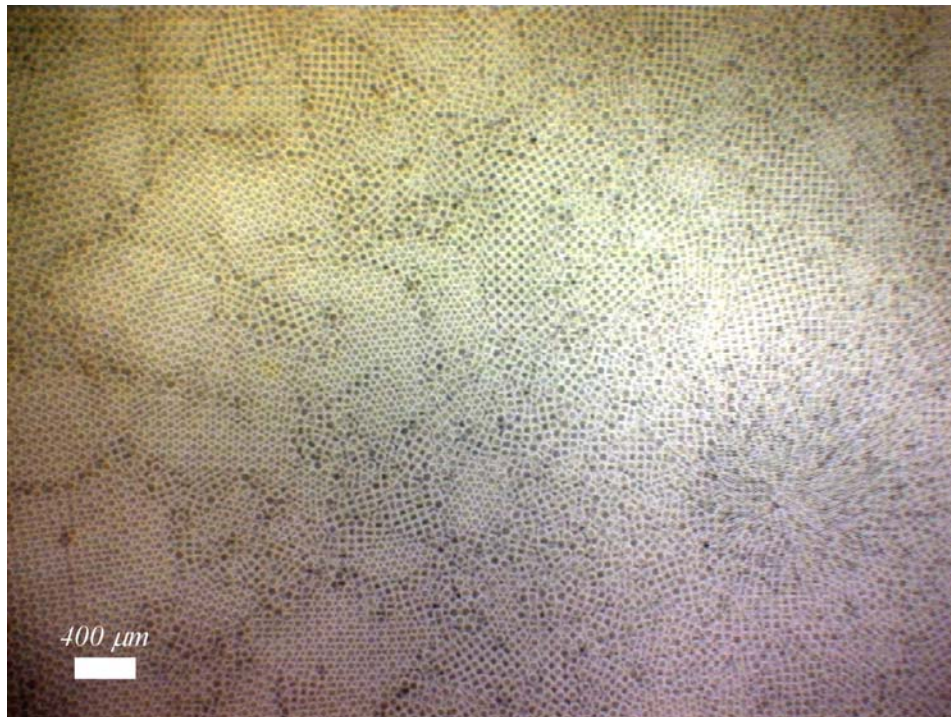


Figure A-1. Aqueous bubbles produced with 50- μm orifice ($Q_l = Q_g = 250 \mu\text{L}/\text{min}$). Fountain is shown at bottom-right of frame.

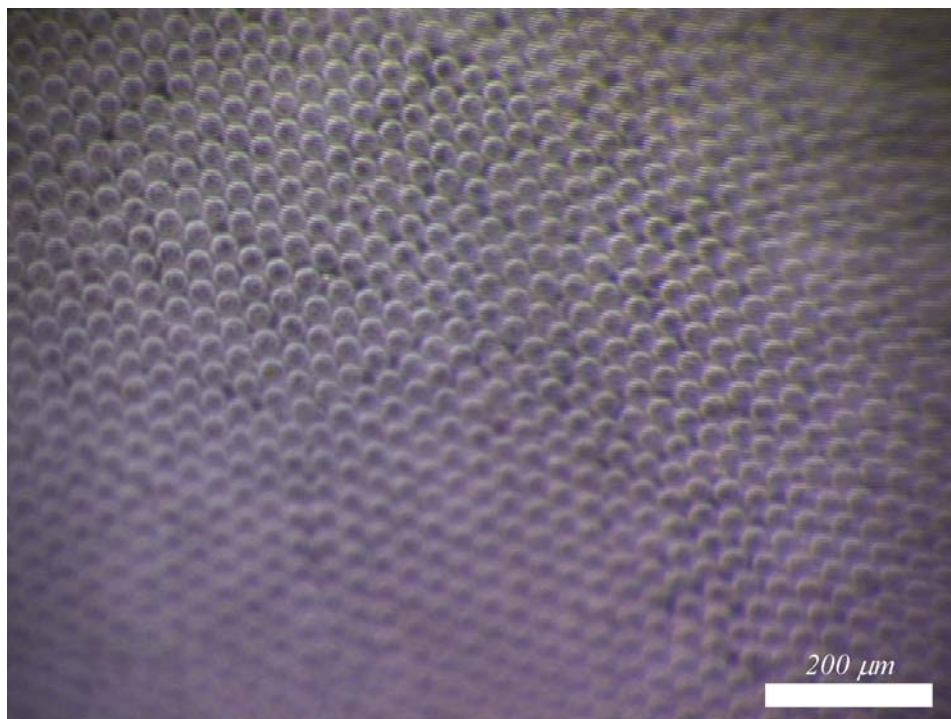


Figure A-2. Aqueous bubbles produced with 50- μm orifice ($Q_l = 250 \mu\text{L}/\text{min}$, $Q_g = 16 \mu\text{L}/\text{min}$).

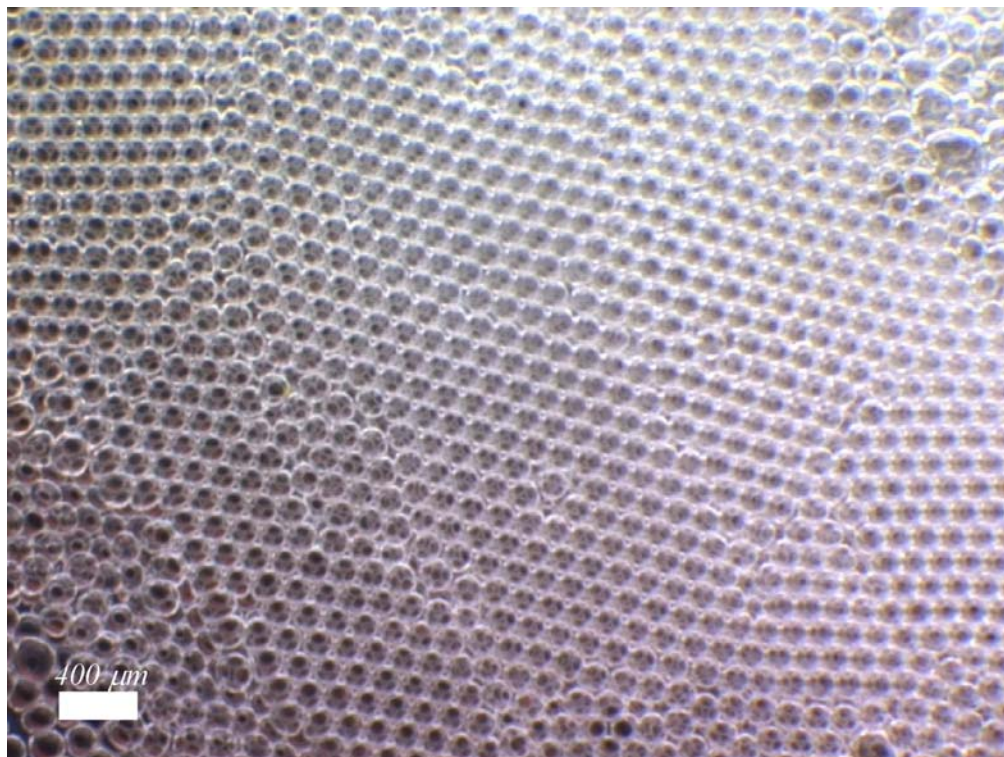


Figure A-3. Acrylamide monodisperse polymeric foam.

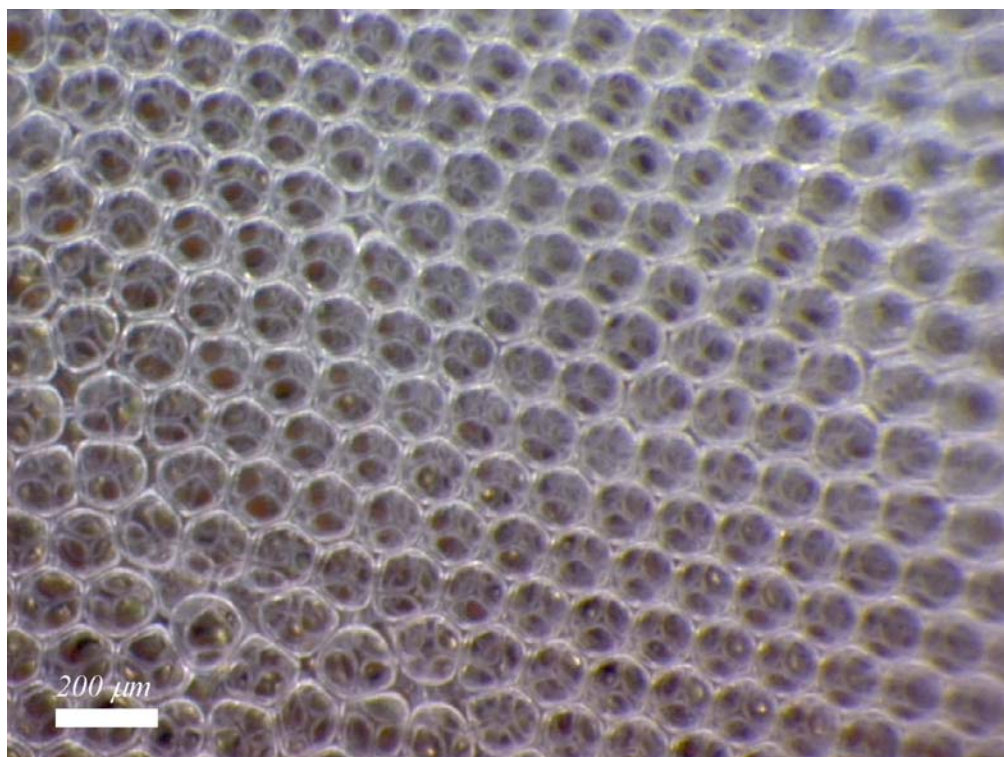


Figure A-4. Acrylamide monodisperse polymeric foam (high magnification).

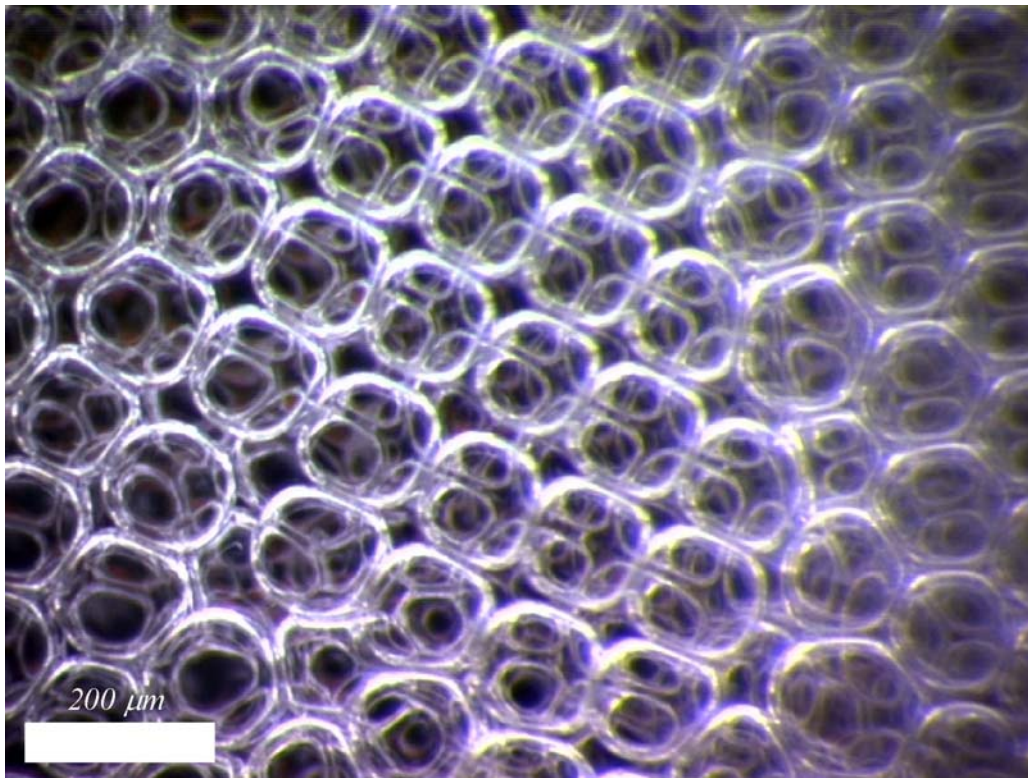


Figure A-5. Acrylamide monodisperse polymeric foam. Image shows preservation of cubic structure in first layer.

NO. OF
COPIES ORGANIZATION

1 DEFENSE TECHNICAL
(PDF INFORMATION CTR
ONLY) DTIC OCA
8725 JOHN J KINGMAN RD
STE 0944
FORT BELVOIR VA 22060-6218

1 US ARMY RSRCH DEV &
ENGRG CMD
SYSTEMS OF SYSTEMS
INTEGRATION
AMSRD SS T
6000 6TH ST STE 100
FORT BELVOIR VA 22060-5608

1 DIRECTOR
US ARMY RESEARCH LAB
IMNE ALC IMS
2800 POWDER MILL RD
ADELPHI MD 20783-1197

3 DIRECTOR
US ARMY RESEARCH LAB
AMSRD ARL CI OK TL
2800 POWDER MILL RD
ADELPHI MD 20783-1197

ABERDEEN PROVING GROUND

1 DIR USARL
AMSRD ARL CI OK TP (BLDG 4600)

NO. OF
COPIES ORGANIZATION

ABERDEEN PROVING GROUND

10 DIR USARL
AMSRD ARL WM
M MAHER
AMSRD ARL WM MA
M VAN LANDINGHAM
D O'BRIEN (3 CPS)
E WETZEL (3 CPS)
AMSRD ARL WM MC
M BRATCHER
T JESSEN